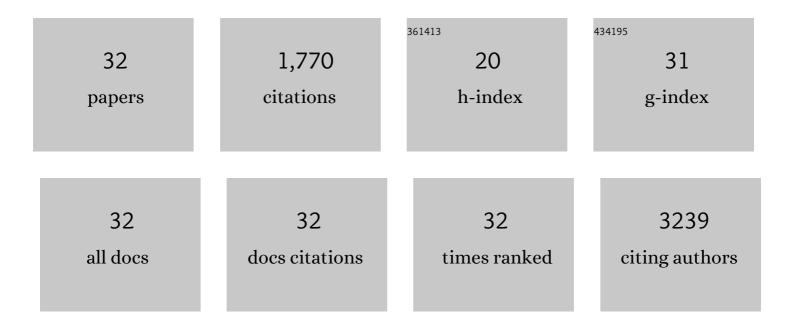
## Shang-Wei Chou

List of Publications by Year in descending order

Source: https://exaly.com/author-pdf/4487911/publications.pdf Version: 2024-02-01



#	Article	IF	CITATIONS
1	In Vitro and in Vivo Studies of FePt Nanoparticles for Dual Modal CT/MRI Molecular Imaging. Journal of the American Chemical Society, 2010, 132, 13270-13278.	13.7	337
2	Prominent Short-Circuit Currents of Fluorinated Quinoxaline-Based Copolymer Solar Cells with a Power Conversion Efficiency of 8.0%. Chemistry of Materials, 2012, 24, 4766-4772.	6.7	329
3	Photothermal cancer therapy via femtosecond-laser-excited FePt nanoparticles. Biomaterials, 2013, 34, 1128-1134.	11.4	116
4	Controlled Growth and Magnetic Property of FePt Nanostructure: Cuboctahedron, Octapod, Truncated Cube, and Cube. Chemistry of Materials, 2009, 21, 4955-4961.	6.7	93
5	Large AuAg Alloy Nanoparticles Synthesized in Organic Media Using a Oneâ€Pot Reaction: Their Applications for Highâ€Performance Bulk Heterojunction Solar Cells. Advanced Functional Materials, 2012, 22, 3975-3984.	14.9	82
6	Synthesis of core/shell metal oxide/polyaniline nanocomposites and hollow polyaniline capsules. Nanotechnology, 2007, 18, 275604.	2.6	72
7	Size-dependent magnetic parameters of fcc FePt nanoparticles: applications to magnetic hyperthermia. Journal Physics D: Applied Physics, 2010, 43, 145002.	2.8	61
8	Antiferromagnetic Iron Nanocolloids: A New Generation in Vivo <i>T</i> <sub>1</sub> ÂMRI Contrast Agent. Journal of the American Chemical Society, 2013, 135, 18621-18628.	13.7	61
9	Sizeâ€Controlled <i>Exâ€nihilo</i> Ferromagnetism in Capped CdSe Quantum Dots. Advanced Materials, 2008, 20, 1656-1660.	21.0	57
10	PtCoFe Nanowire Cathodes Boost Shortâ€Circuit Currents of Ru(II)â€Based Dyeâ€Sensitized Solar Cells to a Power Conversion Efficiency of 12.29%. Advanced Functional Materials, 2018, 28, 1703282.	14.9	55
11	Surfactant-Directed Synthesis of Ternary Nanostructures: Nanocubes, Polyhedrons, Octahedrons, and Nanowires of PtNiFe. Their Shape-Dependent Oxygen Reduction Activity. Chemistry of Materials, 2012, 24, 2527-2533.	6.7	53
12	Tri-iodide Reduction Activity of Shape- and Composition-Controlled PtFe Nanostructures as Counter Electrodes in Dye-Sensitized Solar Cells. Chemistry of Materials, 2016, 28, 2110-2119.	6.7	51
13	A Versatile Theranostic Delivery Platform Integrating Magnetic Resonance Imaging/Computed Tomography, pH/ <i>cis</i> -Diol Controlled Release, and Targeted Therapy. ACS Nano, 2016, 10, 5809-5822.	14.6	49
14	Fluorinated thienyl-quinoxaline-based D–π–A-type copolymer toward efficient polymer solar cells: synthesis, characterization, and photovoltaic properties. Polymer Chemistry, 2013, 4, 3411.	3.9	46
15	One-step synthesis of degradable T <sub>1</sub> -FeOOH functionalized hollow mesoporous silica nanocomposites from mesoporous silica spheres. Nanoscale, 2015, 7, 2676-2687.	5.6	43
16	Uniform size and composition tuning of PtNi octahedra for systematic studies of oxygen reduction reactions. Journal of Catalysis, 2014, 309, 343-350.	6.2	41
17	Shape-Dependent Light Harvesting of 3D Gold Nanocrystals on Bulk Heterojunction Solar Cells: Plasmonic or Optical Scattering Effect?. Journal of Physical Chemistry C, 2015, 119, 7554-7564.	3.1	36
18	Engineering of Single Magnetic Particle Carrier for Living Brain Cell Imaging: A Tunable T <sub>1</sub> -/T <sub>2</sub> -/Dual-Modal Contrast Agent for Magnetic Resonance Imaging Application. Chemistry of Materials, 2017, 29, 4411-4417.	6.7	34

SHANG-WEI CHOU

#	Article	IF	CITATIONS
19	Oneâ€Step, Roomâ€Temperature Synthesis of Glutathioneâ€Capped Ironâ€Oxide Nanoparticles and their Application in In Vivo <i>T</i> <sub>1</sub> â€Weighted Magnetic Resonance Imaging. Small, 2014, 10, 3962-3969.	10.0	30
20	Infrared-active quadruple contrast FePt nanoparticles for multiple scale molecular imaging. Biomaterials, 2016, 85, 54-64.	11.4	26
21	Comprehensive study of medium-bandgap conjugated polymer merging a fluorinated quinoxaline with branched side chains for highly efficient and air-stable polymer solar cells. Journal of Materials Chemistry A, 2014, 2, 20203-20212.	10.3	17
22	Low-toxicity FePt nanoparticles for the targeted and enhanced diagnosis of breast tumors using few centimeters deep whole-body photoacoustic imaging. Photoacoustics, 2020, 19, 100179.	7.8	15
23	Strategic Design of Three-Dimensional (3D) Urchin-Like Pt–Ni Nanoalloys: How This Unique Nanostructure Boosts the Bulk Heterojunction Polymer Solar Cells Efficiency to 8.48%. Chemistry of Materials, 2014, 26, 7029-7038.	6.7	13
24	Mesoporous Silica Promoted Deposition of Bioinspired Polydopamine onto Contrast Agent: A Universal Strategy to Achieve Both Biocompatibility and Multiple Scale Molecular Imaging. Particle and Particle Systems Characterization, 2017, 34, 1600415.	2.3	13
25	Alloy Nanostructured Catalysts for Cathodic Reactions in Energy Conversion and Fuel Generation. Energy & Fuels, 2021, 35, 18857-18870.	5.1	8
26	Enhancing the Catalytic Activity of Tri-iodide Reduction by Tuning the Surface Electronic Structure of PtPd Alloy Nanocrystals. Journal of Physical Chemistry C, 2019, 123, 12722-12729.	3.1	7
27	One-Pot Synthesis of Highly Emissive, Green-to-Red (ZnS) <i><sub>x</sub></i> -Cu <sub>0.1</sub> InS <sub>1.55</sub> /ZnS Core/Shell Nanoparticles via Surfactant Induced Nucleation Process. Materials Express, 2012, 2, 224-232.	0.5	6
28	Silver nanoprism-based paper as a ratiometric sensor for extending biothiol detection in serum. New Journal of Chemistry, 2017, 41, 15120-15126.	2.8	5
29	Engineered core–shell magnetic nanoparticle for MR dual-modal tracking and safe magnetic manipulation of ependymal cells in live rodents. Nanotechnology, 2018, 29, 015102.	2.6	5
30	Boost reactivity of tri-iodide reduction electrode by highly faceted octahedral PtNi nanocrystals. Journal of Catalysis, 2021, 396, 297-303.	6.2	5
31	Direct evidence of type II band alignment in nanoscale P3HT/CdSe heterostructures. Nanotechnology, 2011, 22, 065202.	2.6	4
32	Solar Cells: PtCoFe Nanowire Cathodes Boost Shortâ€Circuit Currents of Ru(II)â€Based Dyeâ€Sensitized Solar Cells to a Power Conversion Efficiency of 12.29% (Adv. Funct. Mater. 3/2018). Advanced Functional Materials, 2018, 28, 1870020.	14.9	0